

# Philae Attitude Determination through Nonlinear Optimal Identification of Solar Arrays Telemetry\*

F. Topputo<sup>a</sup>, G.M. Caputo<sup>a</sup>, and F. Bernelli-Zazzera<sup>a</sup>

<sup>a</sup>Politecnico di Milano, Dept. of Aerospace Science and Technology  
Via La Masa, 34 – 20156, Milano, Italy

## Abstract

In Rosetta lander Philae, the ability to increase the on-comet power production gives the chance to maintain the system alive, as well as the opportunity to accomplish scientific experiments during the Long Term Science (LTS) phase. This can be accomplished if the lander operates at solar incidence angles that maximize the total power produced by the solar arrays. However, due to strict mass limitations, the lander lacks of systems for attitude determination. In this work, a method based on system identification and parameter estimation has been developed to reconstruct the Sun orbit relative to Philae in on-comet conditions. The objective is to find the azimuth and elevation angles of the Sun as a function of time, which is done by post-processing the telemetry data acquired few hours after landing. This allows us to design the optimal rotation of Philae to maximize the power produced, and thus the scientific return.

## 1. Introduction

The Rosetta mission has been developed by the European Space Agency (ESA) with the objective to investigate a comet nucleus. Started in 1993, one of the Agency's cornerstone missions in Horizon 2000 program, Rosetta's main tasks are: 1) the global characterization of comet's nucleus and surface topography; 2) the characterization of chemical and mineralogical composition, and the isotopic relations; 3) the derivation of physical properties of comet's nucleus [1]. Launched on 2 March 2004 on an Ariane 5 rocket, the spacecraft will rendezvous in 2014 with the target comet 67P Churyumov-Gerasimenko. Gathered informations present a comet's diameter of around 4 km and a rotational period of about twelve hours [2].

The on-comet analysis will be performed by Philae, the comet lander [3, 4]. The lander is separated once the comet is reached, after the landing trajectory and site are defined. Once landed, the only degree of freedom is the rotation around the zenith axis (see Figure 1), although there is a limited possibility to tilt and lift the lander main body. The total mass is about 100 kg, and most of the surface is covered with solar cells whose aim is to feed the Power Sub-System (PSS) to charge the secondary battery [5]. The lander main operative phases are Separation, Descent, and Landing (SDL), First Science Sequence (FSS) and Long Term Science (LTS). The first two phases last for

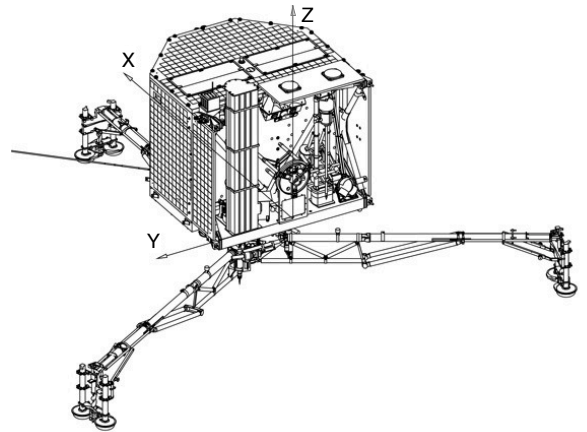


Figure 1. Philae configuration after deployment.

five comet days after the separation from Rosetta, and their power demand is satisfied by the primary battery. The LTS duration will depend upon the capacity of generating electrical power with the solar arrays [10].

As Philae is detached, power provision is given by a Battery unit, consisting of a Primary and Secondary unit, and the Solar Arrays (SA). The SDL and FSS will relay on the Primary Battery, with capacity of 1200 Wh at BoL (1000 Wh at EoL), while the LTS will depend on the Secondary Battery, 150 Wh at BoL (130 Wh at EoL), which is rechargeable through the SA [5]. This configuration is adopted to make it pos-

\*Based on paper presented at the XXII Congresso Nazionale AIDAA, September 2013 Naples, Italy

<sup>1</sup>©AIDAA, Associazione Italiana di Aeronautica e Astronautica

sible executing the Long Term Science (LTS). This maximizes the scientific return of the mission as the comet approaches the perihelion. Indeed, the approximately 2 m<sup>2</sup> SA will produce about 8 W of peak power. This is achieved with Low-Intensity Low-Temperature (LILT) solar cells, placed on six different faces of Philae (see Figure 2). The total number of silicon solar cells is 1224 with dimension of 32.4 mm x 33.7 mm, 200 μm thick; the cell efficiency is approximately 19% in LILT conditions [6]. Power distribution is performed via the Lander Primary Bus (non-stabilized, +28 V baseline) [7]. The architecture chosen for the electrical subsystem is the Maximum PowerPoint Tracking (MPPT) [8].

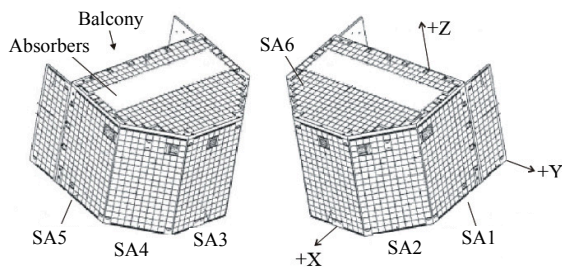


Figure 2. Philae SA distribution.

During the LTS the ability to increase the on-comet power production gives the chance to maintain the system alive, as well as the opportunity to accomplish additional scientific experiments. This can be done if the lander operates at solar incidence angles that maximize the total power produced by the solar arrays. However, due to strict mass limitations, the lander lacks of systems for attitude determination.

In this work, a method based on system identification and parameter estimation has been developed to reconstruct the orbit of the Sun relative to Philae in on-comet conditions. The objective is to find the azimuth and elevation angles of the Sun as a function of time. This is done by post-processing the telemetry data acquired few hours after landing.

**2. Statement of the problem**

The ability to increase the power production is twofold: it gives the chance to maintain the system alive and it enables executing the scientific experiments of the LTS, provided that the power exceeds the threshold of about 5.5 W, which is needed to keep Philae on. This requires operating at solar incidence angles that maximize the total power production. The

Sun incidence angles define the Sun orientation in the Philae coordinate system: the azimuth  $\alpha$ , defined as the horizontal angle measured clockwise from the Y axis to the perpendicular projection of the Sun onto the local horizon; the elevation  $\beta$ , the angle between the Sun and the local horizon (see Figure 3). The azimuth angle ranges from 0 to 360°, while the elevation varies within -90° and 90°.

The aim is to reconstruct the trajectory of the Sun from the PSS telemetry. The six solar panels are connected to the bus via five MPPT; SA1 and SA5 have in common the same tracker as they never expose to the direct sunlight simultaneously. The telemetry reports the MPPT output currents [mA] and their times [s], as well as the SA input voltages [V] and their times [s] (see Figure 4).

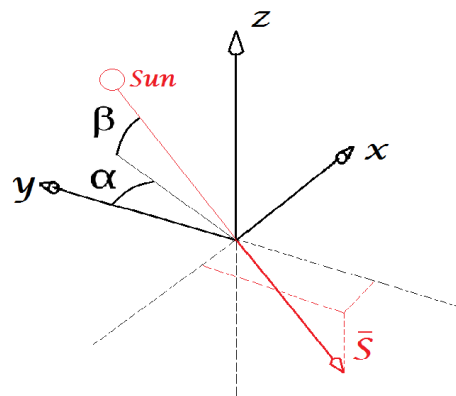


Figure 3.  $\alpha$  and  $\beta$  with  $\mathbf{S}$  in Philae body reference system.

The requirement is an algorithm capable of obtaining the Sun incidence angles within the timeframe resolved in the PSS telemetry. As the model that describes the power generation of the lander SA is known, this procedure should be able to find the variables that produced the telemetry data through an optimization step. The final result is the rotation angle required to point towards the direction of maximum power production during the cometary day.

**3. Preconditons**

It is assumed that only the direct sunlight contributes to the SA power production. Also, the SA surfaces are considered clean from any deposition with all the cells properly working. The landing site is considered flat with zero inclination of the lander with

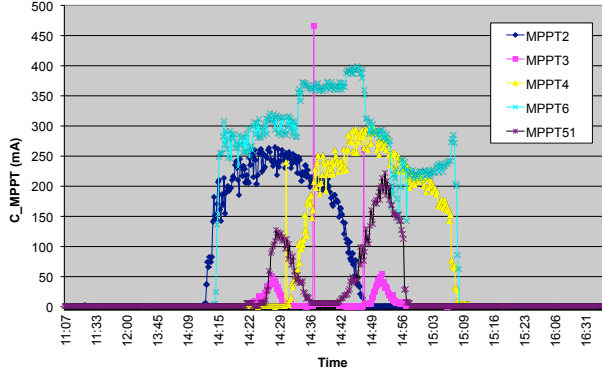


Figure 4. MPPT output current during the power system test [9].

respect to the local normal. Due to the lack of telemetry data needed to test the algorithm with, an MPPT simulator is developed. This takes as input the Sun incidence angles and creates a corresponding power telemetry file lookalike [7].

### 3.1. Data preprocessing

As the current outputs are sampled at about every 4:15 min ( $3.9 \times 10^{-3}$  Hz) and the frequency at which the MPPTs operate is on the order of kHz, it is not possible to determine a common behavior in the signal. A way to reduce such effect is *smoothing*. In smoothing, the data points of a signal are modified so that individual points that are higher than the immediately adjacent points (presumably because of noise) are reduced, and points that are lower than the adjacent points are increased. This naturally leads to a smoother signal. As long as the true underlying signal is actually smooth, then the true signal will not be much distorted by smoothing, but the noise will be reduced.

The *triangular smoothing* method is chosen, where each data point  $Y_j$  is replaced by  $S_j$ , the weighted average of the five adjacent points

$$S_j = \frac{Y_{j-2} + 2Y_{j-1} + 3Y_j + 2Y_{j+1} + Y_{j+2}}{9}, \quad (1)$$

$$j = 2, \dots, n - 2,$$

where  $n$  is the total number of samples [11] (see Figure 5).

If the noise in the data is “white noise” (that is evenly distributed over all frequencies and actually resemble our case) and its standard deviation is  $s$ , then the standard deviation of the noise remaining in the signal after the first pass of an unweighted sliding-average smooth will be approximately  $\sqrt{s/m}$  where  $m$  is the smooth width [11].

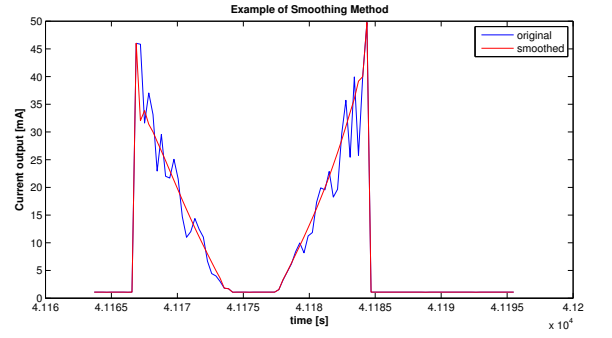


Figure 5. Example of *triangular smoothing* (20 samples) on a current output.

### 3.2. Time windows identification

The determination of the Sun incidence angles depends on the combination of illuminated panels. As only some panels can be illuminated in a certain period, it is important to identify intervals of time, defined as time windows, where only some arrays are actually working: these windows begin and end as one or more panels starts or stops producing power. They include time samples in which only a certain combination of panels are producing a relevant current output, where others with less significant output are discarded.

Each current output value has different sampling time due to the fact that the data logger reads one MPPT at a time. Thus, the time windows, to be correctly defined, need all the samples to refer at the same time grid. A linear interpolation is then performed to refer all the values to a common time grid. The reference time is that of SA2, this one being the first to be sampled at each cycle.

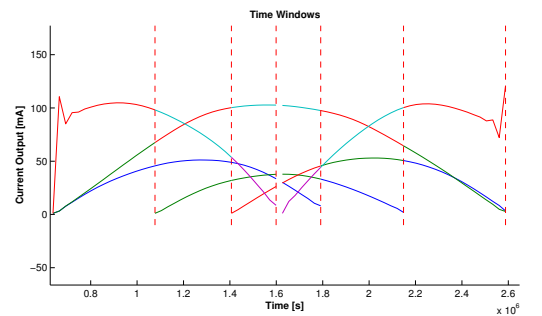


Figure 6. Example of Time Windows during a cometary day.

### 3.3. First guess definition

A first guess definition is used to achieve a faster convergence and to avoid finding possible local minima during the optimization process. This is computed through linear approximation, and all the second-order effects are included in the efficiency coefficient. The  $\alpha$  and  $\beta$  angles of the Sun direction in Philae reference body system are obtainable from the Sun vector composed by three components:  $S_x, S_y, S_z$ . The general scalar equation for the power output for a solar array is

$$P = V I = A \mathbf{n} \cdot \mathbf{S} \eta, \quad (2)$$

where  $P$  is the power output;  $V, I$  are the voltage, current at which the panel operates,  $A$  is the total area of the solar array,  $\mathbf{n}$  is the solar panel normal,  $\mathbf{S}$  is the Sun direction vector ( $\mathbf{S} = S\mathbf{s}$ , where  $\mathbf{s}$  is the Sun unit vector and  $S$  is the sunlight intensity), and  $\eta$  is the total efficiency, which includes MPPT and SA efficiency, SA temperature, dust/ice deposition, etc.

By writing (2) for  $n$  panels, a system is obtained,

$$\mathbf{P} = 28 \mathbf{I} = \mathbf{A} \mathbf{N} \mathbf{s} S \eta, \quad (3)$$

with

$$\mathbf{P} = \begin{bmatrix} P_1 \\ \vdots \\ P_n \end{bmatrix}, \quad \mathbf{I} = \begin{bmatrix} I_1 \\ \vdots \\ I_n \end{bmatrix}, \quad \mathbf{A} = \begin{bmatrix} A_1 & \cdots & 0 \\ \vdots & \ddots & \vdots \\ 0 & \cdots & A_n \end{bmatrix},$$

$$\mathbf{N} = \begin{bmatrix} N_{1x} & N_{1y} & N_{1z} \\ \cdots & \cdots & \cdots \\ N_{nx} & N_{ny} & N_{nz} \end{bmatrix}, \quad \mathbf{s} = \begin{bmatrix} s_x \\ s_y \\ s_z \end{bmatrix}.$$

$\mathbf{P}$  is a vector containing the power outputs,  $\mathbf{I}$  is a vector of currents (from the telemetry),  $\mathbf{N}$  is a matrix containing as rows the normals of the panels lit, and  $\mathbf{A}$  is a matrix with diagonal the vector of the total area of the lighted solar arrays. Equation (3) is written at the  $I$ - $V$  curve maximum power point and already considers the 28 V bus voltage.

To invert (3),  $\mathbf{N}$  is required to be invertible. This means taking in consideration only three panels at a time. Also, the geometry is such that SA6 must be always included, otherwise the column of  $\mathbf{N}$  with  $z$  components is always empty. By inverting (3) we find the Sun unit vector

$$\mathbf{s} = \frac{28}{S\eta} (\mathbf{A} \mathbf{N})^{-1} \mathbf{I}. \quad (4)$$

Given  $\mathbf{s}$ , it is possible to recover  $\alpha$  and  $\beta$  as

$$\alpha = \begin{cases} \arctan\left(\frac{s_x}{s_y}\right) & \text{if } s_y \geq 0, \\ \arctan\left(\frac{s_x}{s_y}\right) + \pi & \text{if } s_y < 0, \end{cases} \quad (5)$$

$$\beta = \arcsin(s_z).$$

When more than three MPPTs have nonzero output, the first guess problem becomes overdetermined: to take advantage of this, it is used a combination system to obtain a series of Sun incidence angle values to lessen the effects of the approximations taken, where the only panel fixed is the lid. A mean value of the first guess is then obtained from the  $\alpha_j$  and  $\beta_j$  obtained.

### 4. Solution of the identification problem

Due to the nonlinear behavior of the system, a solution to the problem is to work with optimization algorithms, specifically through parameter estimation. This is capable to determine the parameters vector of a system  $\mathbf{p}$  from the values of the observed state, typically represented from a system of ordinary differential equations,

$$\dot{\mathbf{y}} = \mathbf{f}[\mathbf{y}(t), \mathbf{u}(t), \mathbf{p}, t], \quad (6)$$

for a given time interval  $t_i \leq t \leq t_f$ , where  $\mathbf{y}$  is the  $n_Y$  dimensional state vector,  $\mathbf{u}$  an  $n_u$  vector of algebraic variables and  $\mathbf{p}$  are the parameters of the system [12]. It is computationally useful to include simple linear bounds on the variables

$$\begin{aligned} \mathbf{y}_l &\leq \mathbf{y}(t) \leq \mathbf{y}_u, \\ \mathbf{u}_l &\leq \mathbf{u}(t) \leq \mathbf{u}_u, \\ \mathbf{p}_l &\leq \mathbf{p} \leq \mathbf{p}_u \end{aligned} \quad (7)$$

The parameter estimation objective function is evaluated at a finite, possibly large, number of discrete points. The goal here is to determine the  $n_p$  dimensional vector  $\mathbf{p}$  to minimize

$$F = \frac{1}{2} \mathbf{r}^T \mathbf{r} = \frac{1}{2} \sum_{k=1}^l r_k^2 \quad (8)$$

with

$$r_k = w_k [y_{i(k)}(\theta_k) - \hat{y}_{i(k)}] \quad (9)$$

where  $y_{i(k)}$  is the state variable  $i$  computed at time  $\theta_k$ ,  $\hat{y}_{i(k)}$  is the observed value at the same time, and  $w_k$  is a possible weight. The time instant  $\theta_k$  must satisfy  $t_i \leq \theta_k \leq t_f$ .

In our problem the parameter to be determined are the Sun incidence angles, and therefore the optimization variable vector is

$$\mathbf{x} = \{\alpha_1, \alpha_2, \dots, \alpha_n, \beta_1, \beta_2, \dots, \beta_n\}. \quad (10)$$

The bounds for  $\alpha$  and  $\beta$  are recovered by the azimuth and elevation range of each panel. Since panels 1 and 5 share the same current output and face opposite direction, their  $\alpha$  values can range from  $0^\circ$  to  $360^\circ$ , and therefore are left out from boundary constraints definition (Table 1). The bounds for  $\beta$  are in Table 2.

Table 1

Bounds for $\alpha$	
Walls	$\alpha$ range
0 0 0	$225^\circ \leq \alpha \leq 315^\circ$
2 0 0	$315^\circ \leq \alpha \leq 360^\circ$
2 3 0	$0^\circ \leq \alpha \leq 45^\circ$
2 3 4	$45^\circ \leq \alpha \leq 135^\circ$
0 3 4	$135^\circ \leq \alpha \leq 180^\circ$
0 0 4	$180^\circ \leq \alpha \leq 225^\circ$

Table 2

Bounds for $\beta$	
Wall	$\beta$ range
6	$-10^\circ \leq \beta \leq 90^\circ$

A nonlinear constrain is obtained by imposing the magnitude of  $\mathbf{s}$  to be 1, i.e.,

$$\mathbf{s}^T \mathbf{s} = s_x^2 + s_y^2 + s_z^2 = 1. \quad (11)$$

which translates into a nonlinear constraint for  $\alpha$  and  $\beta$ ,

$$g(\mathbf{x}) = (\cos(\beta) \sin(\alpha))^2 + (\cos(\beta) \cos(\alpha))^2 + (\sin(\beta))^2 - 1 = 0. \quad (12)$$

The residual vector  $\mathbf{r}_i$  at time  $t_i$  is the difference between the MPPT output current from the telemetry ( $\hat{\mathbf{y}}_i$ ) and the reconstructed one ( $\mathbf{y}_i$ ), i.e.,

$$\mathbf{r}_i = \mathbf{y}_i - \hat{\mathbf{y}}_i. \quad (13)$$

The dependence of the performance index to the parameters vector  $\mathbf{x}$  is through the reconstructed MPPT current outputs. This is achieved through the model present in PSAS [7], the wall temperature models [13], and the end-of-life total radiation dose. Once the current output is simulated, the performance index is computed as

$$F(\mathbf{x}) = \sum_{i=1}^n (\mathbf{y}_i - \hat{\mathbf{y}}_i)^T (\mathbf{y}_i - \hat{\mathbf{y}}_i). \quad (14)$$

The performance index must also account for the MPPT power conversion loss. To avoid problems arising from the discrepancy between solution and telemetry a correction factor is included, i.e.

$$F(\mathbf{x}) = \sum_{i=1}^n (\hat{\mathbf{y}}_i - \hat{\mathbf{y}}_i/0.8)^T (\hat{\mathbf{y}}_i - \hat{\mathbf{y}}_i/0.8). \quad (15)$$

It is now possible to write the nonlinear parameters estimation problem as follows

$$\min_{LB \leq \mathbf{x} \leq UB} F(\mathbf{x}) \quad \text{subject to} \quad g(\mathbf{x}) = 0. \quad (16)$$

It is interesting to show a possible trend of the performance index computed as function of azimuth  $\alpha$  and elevation  $\beta$  at a defined sampling time (Figure 7).

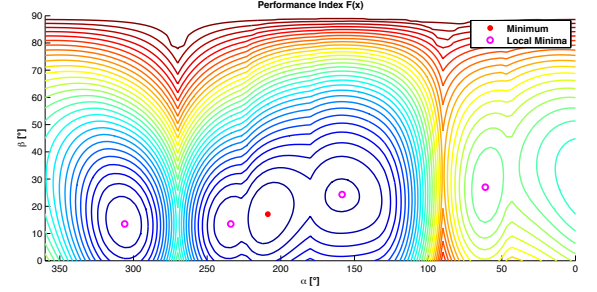


Figure 7. Performance index contours.

## 5. Results

The simulation architecture starts from a series of different Sun incidence angles, used to create the relative Power telemetry files through the MPPT simulator. These are used to test the algorithm by comparing the results with the initial parameters, through different kind of cometary days and locations along the comet surface [14].

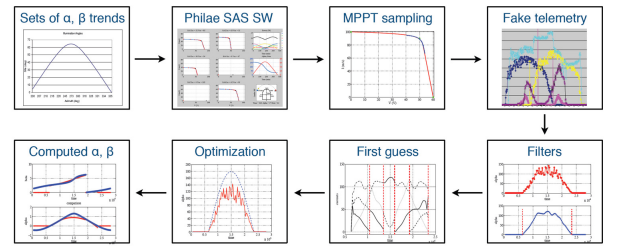


Figure 8. Simulation Architecture

Once the direction of maximum power production,  $\bar{\alpha}$ , is inferred from the reconstructed Sun orbit, the rotation required to maximize the power production is computed through

$$\alpha_R = \begin{cases} 90 - \bar{\alpha} & \text{if } 0 \leq \bar{\alpha} \leq 270^\circ \\ 360 - (\bar{\alpha} - 90) & \text{if } 270^\circ < \bar{\alpha} < 360^\circ \end{cases}$$

In this way the rotation is always less than  $180^\circ$ .

### 5.1. Regular Cometary day

A regular cometary day is characterized by the presence of the night, the sunrise and the sunset at each comet revolution. The  $\beta$  angle is positive during the day. In this situation the Sun culmination, defined by the maximum value achieved by  $\beta$ , determines the maximum power direction  $\bar{\alpha}$ , as the azimuth coupled to  $\bar{\beta} = \max(\beta)$ .

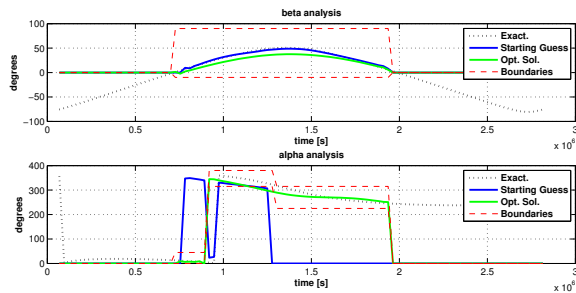


Figure 9. Regular day: exact and computed solutions.

It is important to notice how, even if the solution is not perfectly overlapping the exact one it is close to it (Figure 9). This entails a rotation that points the lander close to the maximum power production attitude, with little loss with respect to optimum condition but a great gain from previous situation.

### 5.2. Summer Polar day

In summer polar conditions, the Sun remains visible during the whole cometary revolution, and there is no night. The maximum power production attitude happens when the wall 3 is directly pointed to the azimuth  $\bar{\alpha}$  coupled to angle of minimum elevation  $\bar{\beta} = \min(\beta)$ . Again, the results are good enough to understand the situation Philae is facing and to operate a correction rotation to significantly increase the power production (Figure 10).

### 5.3. Zenith Transit

In this situation the Sun intersects the Philae zenith direction. As the Sun transits over the lander,  $\beta$  reaches maximum value ( $\pi/2$ ) and  $\alpha$  jumps of  $\pi$ . In this scenario the direction of maximum power production is defined by the azimuth  $\bar{\alpha}$  placed midway from the azimuth relative to sunrise  $\alpha_{rise}$  to the one related to sunset  $\alpha_{set}$ , along the arc covered by the Sun during the cometary day.

In this situation the results are not as good as in the previous ones. The elevation is not close to the exact one, and the azimuth has an acceptable trend but still not perfect. Nevertheless, through critical analysis it is possible to understand the situation and to operate

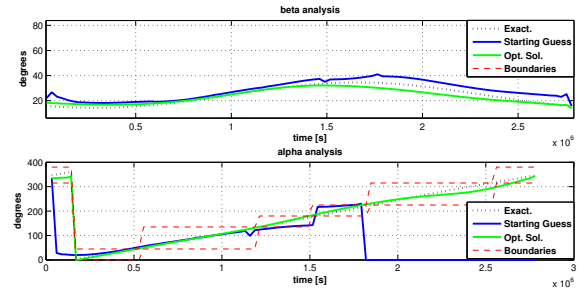


Figure 10. Summer polar: exact and computed solutions.

consequently the lander. Thanks to jump in the  $\alpha$  solution near the maximum point of  $\beta$  is possible to recognize the zenith transit condition. The sunrise and sunset azimuths are recovered by comparing the starting guess and solution [15].

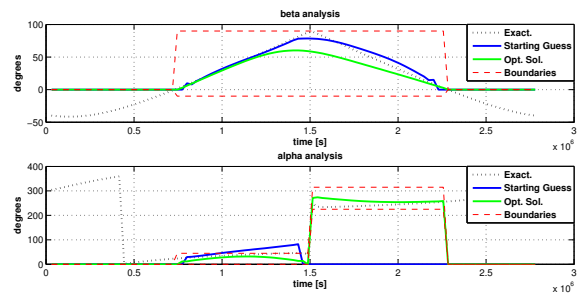


Figure 11. Zenith transit: exact and computed solutions.

## 6. Conclusions

This paper presents an algorithm capable to find the optimum power production orientation needed by the Rosetta lander Philae on comet 67P-Churyumov-Gerasimenko, so to increase the mission life expectation during LTS operative phase. As the lander is not provided with any kind of attitude determination instruments, this is done by analyzing the power telemetry file obtained during the first days on the comet.

By using the models for the solar arrays power production, a nonlinear optimization problem is defined so to recover the Sun incidence angles time histories defined as  $\alpha$ , azimuth, and  $\beta$ , elevation, in the lander reference system, starting from the MPPT current output samples. Once the angles are obtained, a correction rotation is computed so to point the lander towards the

maximum power production direction, where such direction depends on the typology of cometary day the lander is facing. As real PSS telemetries are not widely available, a simulator capable to provide MPPT current outputs starting from Sun incidence angles time histories has been created. Such telemetries are then used to test the algorithm during all possible case scenarios, covering every kind of cometary day and location over its surface.

## REFERENCES

1. K.-H. Glassmeier, H. Boehnhardt, D. Koschny, E. Kührt, I. Richter, "The Rosetta Mission: Flying Towards the Origin of the Solar System ", *Space Science Reviews*, Vol. 128, No. 1–4, 2007
2. P. Lamy, I. Toth, H. Weaver, L. Jorda, M. Kaasalainen, and P. Gutiérrez, "Hubble Space Telescope Observations of the Nucleus and Inner Coma of Comet 67P/Churyumov-Gerasimenko ", *Astronomy & Astrophysics*, Vol. 458, 2006
3. J.-P. Bibring et al, "The Rosetta Lander Philae Investigations ", *Space Science Reviews*, Vol. 128, No. 1–4, 2007
4. S. Ulamec et al, "Rosetta Lander - System Status after Five Years in Space ", *Aerotecnica Missili e Spazio* Vol. 88, No. 4, 2009
5. F. Topputo, F. Bernelli-Zazzera, A. Ercoli-Finzi, "On-Comet Power Production: the Case of Rosetta Lander Philae", *Proceedings of the European Planetary Science Congress 2010*, Vol. 5, EPSC2010-96, Rome, September 2010
6. S. Brambillasca, F. Topputo, A. Ercoli-Finzi, and R. Campesato, "LILT Measurement on Silicon Solar Cells of Rosetta Lander Philae ", *XX AIDAA Congress*, Milano, Italy, June 29?July 3, 2009
7. F. Topputo, F. Bernelli-Zazzera, F. Ercoli-Finzi, "Solar Array Simulators for Low Power Space Missions", *Proceedings of the 3rd CEAS Air & Space Conference*, 2011
8. VV. AA., "Lander User Manual: 2.2-9b Solar Arrays ", *Report RO-LAN-UM-3100-SA*, 2007
9. M. Maibaum, "Report on Power System Test Operations ", *Report RO-LAN-RP-30445*, 2010
10. S. Ulamec, J. Biele, "From the Rosetta Lander Philae to an Asteroid Hopper: lander concepts for small bodies missions", *7th International Planetary Probe Workshop 7*, Barcelona, 2010
11. J.S. Simonoff, "Smoothing Methods in Statistics ", Springer, 1998
12. J.T. Betts, "Practical Methods for Optimal Control and Estimation Using Nonlinear Programming", Siam, 2010
13. J. Biele, "Philae Solar generator models ", *Technical Note RO-LAN-TN-3013-JBI*, 2005
14. G. Pinzan, "Landing site selection for Rosetta lander Philae through a multidisciplinary approach", *MSc Thesis*, Politecnico of Milano, 2012
15. G.M. Caputo, "On-comet attitude determination of Rosetta lander Philae through nonlinear optimal system identification", *MSc Thesis*, Politecnico of Milano, 2012
16. M. Pesco, A. Ercoli-Finzi, "Rosetta Space Mission The Solar Array Photovoltaic Assembly ", *XIX Congresso Nazionale AIDAA*, September 2007, Forlì, Italy